Engineering Solid Mechanics 11 (2023) 411-418

Contents lists available at GrowingScience

Engineering Solid Mechanics

homepage: www.GrowingScience.com/esm

Experimental analysis of spliced joint connections in GFRP short column

M. J. Srujan[a] and Seelam Srikanth[b*]

[a]*Ph.D. Scholar, School of Civil Engineering, REVA University, Bangalore-560064, Karnataka, India*
[b]*Associate Professor, School of Civil Engineering, REVA University, Bangalore-560064, Karnataka, India*

ARTICLEINFO

Article history:
Received 10 April 2023
Accepted 16 May 2023
Available online
16 May 2023

Keywords:
GFRP
Spliced connection
Short column
Axial load

ABSTRACT

This paper describes an experimental program developed to investigate non-bearing spliced composite short column connections made of Glass Fiber Reinforced Polymer (GFRP) that are subjected to axial loading. This study provides aspects such as the load-bearing capacity of the connection, failure modes, load distribution in the connection, displacement in the joint, stiffness, and compressive strength. The design of the joint in this study that connects two 350mm GFRP H-sections to form a short column connection is based on euro codes BS EN 1990 and BS EN 1991, which are used to design steel splicing connections for beams and columns. Four design specifications models are made depending on the positioning of the cover plates in the inner flange, outer flange, and web region of the H-sections to examine the requirement of a specific cover plate, and the H-sections are bolted to each other using M8 8.8 grade steel bolts. The samples tested in this study indicated a dominant failure in the flange region, with model-4 providing 92.83% compressive strength when compared to an uncut GFRP short column.

1. Introduction

Fiber Reinforced Polymer (FRP) is a reinforced polymer composite material that is widely used in the aeronautical and aerospace industries but is gaining popularity in the construction industry due to its lightweight and high load-bearing capacity for the same area that traditional steel used in construction occupies (Frigione & Lettieri, 2018). Because of their high strength-to-weight ratio, these materials were introduced into the construction industry as retrofitting counterfeits used to restore or strengthen weaker structures (Ferdous et al., 2021). There are various types of FRPs and the most popular one amongst them is GFRP which is a Glass fiber and epoxy composite because of its low cost of production compared to other FRPs such as CFRP or AFRP. Using GFRP in the construction industry has several advantages, including its non-conductivity of heat, electricity, and magnetism, non-corrosive nature, rot-free abilities, lightweight, and so on. These advantages will lead to advancements in construction and will have consequences in other industries as well, but the material is not being used to its full potential due to a lack of design codes (Kim, 2019). GFRPs, unlike traditional steel and iron, cannot be welded but can be bolted, riveted, and bonded to form connections (Al-Rubaye et al., 2020). Bolts and rivets used in GFRP structures are typically made of steel and iron, but the use of GFRP bolts to establish homogeneous connections is becoming popular, complementing the use of the material throughout the structure. A monolithic reinforcement or load-bearing structure is preferable to a cut or fragmented component for construction, but transporting a single large piece of material becomes tedious and expensive and is not considered ideal in most situations (Bazli et al., 2020). As a result, a connection design that provides the structure with the same strength, load-bearing capacity, and other benefits as an uncut piece would when used in real-time is required.

The use of GFRP in the construction industry has numerous advantages, and when compared to its naturally occurring replacement counterparts like wood or steel, the issues of depletion, extinction, extraction, deforestation, and so on are all

* Corresponding author.
E-mail addresses: srikanths.reddy@reva.edu.in (S. Srikanth)

ISSN 2291-8752 (Online) - ISSN 2291-8744 (Print)

doi: 10.5267/j.esm.2023.5.003

resolved (Sheikh & Li, 2007; Vedernikov et al., 2020). In earthquake-prone areas, wood is preferred over steel because of its ability to absorb or dampen vibrations, whereas steel transmits and resonates with vibration, causing structural issues (Fahmy, 2013). In addition, steel-reinforced structures require fewer plastic hinges to withstand dynamic loading than traditional live load, dead load, wind load, snow load, and so on. This problem is solved by adding reinforcement and using larger cross-sectional structures, which increases dead load and makes the structure heavy. In earthquake-prone areas, GFRPs can be used in place of steel to create a static and practical structures (Tempelman, 2014). GFRP, like wood, has the benefit of dampening vibration due to the material being stiff and less tensile. GFRP also has a significantly higher thermal capacity and is rot-free when compared to wood. As a result, GFRP has the potential to replace wood, steel, aluminum, titanium, and other construction materials in the construction of standard- or mega-structures (Wallace, 1965). Another common practice in the construction industry is to provide structures with composite materials that contrast each other's flaws, such as in RCC, where concrete is used for compressive strength and steel for tensile strength. This aspect of using composite structures can be traced back to when wood and clay were popular building materials. Composite connections are ideal for enhancing the ability of one material by compensating for redundancies in the other (Shin et al., 2019). Because of its numerous advantages over other construction materials, GFRP is widely used as a composite material for the construction of military-grade and other mega-structures such as oil refineries, bridges, industrial harbours, and so on (Harley et al., 2017; Phan Viet et al., 2020).

GFRP H-section connections are bonded, bolted, and riveted, as compared to steel H-section connections, which can be bolted, riveted, and welded. This raises the question of which type of connection is the strongest; what constitutes a strong GFRP connection; can composite connections provide adequate strength; and what is the most commonly used connection in I-sections and H-sections (Zhao & Zhang, 2007; Viet et al., 2021). Splicing is a common connection used in steel structures to connect two H-sections or I-sections. The splicing connection's popularity is due to its ability to provide stiff continuity, strength, toughness, and firmness across the section of the connection (Nhut et al., 2022). Splicing is a method of connecting two horizontal or vertical structures such as I-sections, H-sections, L-sections, T-sections, and so on. Splicing can be done in GFRP H-sections as well as steel, and the two most common types used to connect H-sections are bearing and non-bearing splicing (Liu et al., 2020). Bearing splicing occurs when two members connected by plates and bolts come into contact with each other, creating a load transfer path directly through the members and the joint. Load transfer does not occur directly through the members in non-bearing splicing because a gap called the splicing gap is maintained between the members to accommodate for any expansion in the joint or to maintain the robustness of the connections (Russo, 2019). As a result, load transfer occurs in non-bearing splicing through the joint or connection members, which in the case of splicing connections are plates and bolts. This helps in understanding the strength of the connection by separating it from the strength of the material in terms of load transfer from one section to another. Because one of the major disadvantages of GFRP is its ability to fail abruptly at maximum loading, having a safety trigger via a splicing gap increases the robustness of the connection, preventing any catastrophes when used in a structure.

The plates used in spliced connections are classified into three types based on their placement: web plates, inner flange plates, and outer flange plates. There are several advantages to using cover plates in different locations of the connection depending on the requirements (Mara, 2016). That is, excessive use of cover plates in a specific location will increase the cost of producing a joint, whereas not using the required amount will result in unsatisfactory connection performance. As a result of the lack of design codes, GFRP is not being used to its full potential in the construction industry, which is increasing the amount of research being done on the material to produce efficient and reliable structures. This study focuses on a significant knowledge gap in GFRP column connections and whether the spliced column has the same strength as an uncut GFRP H-section by performing the lab tests.

2. Experimental program

The test subjects are made of two GFRP H-sections, each of which is 350mm long and has an H-dimension of 150 × 76 × 6.5 mm. The guidelines for non-bearing splice connection design is derived from euro codes (BS EN, 1990; BS EN, 1991). Four models are developed based on the presence of cover plates in the inner flange, outer flange, and web region, as shown in figure 1. According to euro code (BS EN, 1993-1-9) guidelines, the diameter of 8 bolt flange connections should be greater than 75% of the total thickness of both inner and outer flange plates combined. The pitch and edge value dimensions for the bolted connection are derived from the width, length, and thickness of the cover plates; for spiced connections using bolts, the pitch (p) distance should be two times the edge (e) distance, ie. p>2e; otherwise, thicker cover plates should be used. The dimensions of the cover plates used to create the models are as follows: the web plate measures 205 × 80 × 5 mm, the inner flange plate measures 420 × 34 × 5 mm, and the outer flange plate measures 410 × 76 × 5 mm. Table 1 shows the pitch and edge values based on these specifications.

Table 1. Splicing connection's edge and pitch values

Cover Plates	Edge-1 (e1) (mm)	Pitch-1 (p1) (mm)	Edge-2 (e2) (mm)	Pitch-2 (p2) (mm)
Inner Flange plate	51.00	102.00	-	-
Outer Flange plate	15	45	51.00	102.00
Web plate	20	40	51.00	102.00

Fig. 1. Designs for model specimens

Model-1 is designed as a simple non-bearing spliced connection with only two steel outer flange plates serving as cover plates, and it is bolted to the two H-sections with 16 M8 steel bolts to form the test sample. Model-2 is built on the same principles as model-1, but instead of two pairs of outer flange plates, two pairs of web plates are used as cover plates, and model-2 is assembled with 20 M8 steel bolts. When model-1 and model-2 are compared, the transfer of load from the web region and the importance of having a web cover plate can be derived due to the presence of a web plate and more bolts in the joint. Model-3 is intended to reinforce the flange region of both H-sections connected by the spicing connection. As a result, two outer flange plates and four inner flange plates are used as cover plates, and a total of 16 M8 bolts are used to form the test samples, allowing a load transfer direction purely through the flange region of the H-section to be determined. Model-4 has the highest number of cover plates and bolts, with 2 outer flange plates, 4 inner flange plates, two web plates, and a total of 20 M8 steel bolts to form the connection. Model-4 is the most reinforced design of the four models, with load transfer occurring in the web and flange region, utilizing the overall H-section. Because the testing is based on the design of a non-bearing spliced connection, each sample has a splicing gap of 25mm. To determine the strength of an un-cut GFRP H-section short column solely on the material property, 350mm length sections are cut and tested to determine the crushing or ultimate load-bearing capacity of the material subjected to axial loading. This provides a baseline against which to calculate the increase or decrease in strength of the connection in comparison to an un-cut structure.

A set of five samples is created and tested for each design, the cover plates and the H-section are clamped onto a drilling table, and holes of 8.5 mm are drilled to accommodate the M8 8.8-grade bolts smoothly using a mechanical drill with a stencil pointing at the bolt locations. According to euro code (BS EN, 15048-1) guidelines, the bolts are tightened to a torque value of 28.84 Nm. The testing guidelines are based on euro code standards for testing connection designs (BS EN, 13706-3), and a total of 25 samples are tested in this study. The fully assembled test sample is installed in an AMSLER compression testing machine that is linked to an Avery 5000kN load cell controlled by hydraulic pressure. To avoid eccentric loading, the test sample is carefully aligned to the centre of the base plate. To measure displacement readings of the specimen when subjected to axial compression, a pair of Linear Variable Differential Transformers (LVDT) are placed on the front and back of the test sample. To record the precise point of failure, ultimate load, and displacement values, the loading rate is set to 0.2 kN/reading. Before testing each sample, the instruments used in this test are checked for proper working conditions and collaborated to zero readings.

3. Results and Discussion

The load versus displacement graphs of the models were plotted based on compression testing machine readings and are shown in Fig. 2. Using the load versus displacement graph, the stiffness value was calculated. The stiffness (K), force per bolt, compressive strength, and bearing stress of the models were calculated and presented in Table 2 and Table 3.

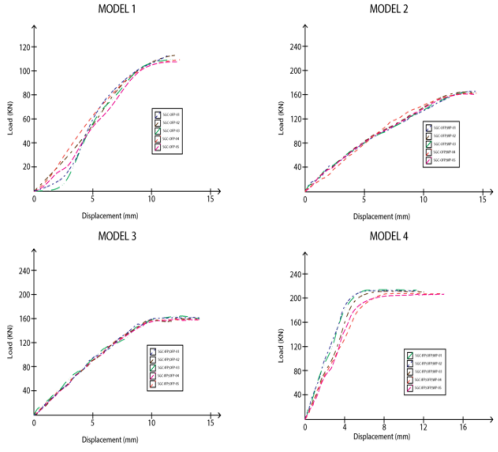

Fig. 2. Load versus displacement graphs of the models

Table 2. Specimen's characteristic properties of model 1 and model 2

Sample ID.	Ultimate load (kN)	Failure displacement (mm)	K (kN/mm)	Force per bolt (kN)	Compressive strength (N/mm^2)	Bearing stress (N/mm^2)	Mode of failure
			Model-1				
SGC-OFP-01	113.20	11.46	16.20	14.15	60.73	276.32	Bearing
SGC-OFP-02	112.70	11.54	16.10	14.09	60.46	275.10	Bearing
SGC-OFP-03	110.30	11.68	15.90	13.79	59.17	269.24	Bearing
SGC-OFP-04	109.50	11.75	15.80	13.69	58.74	267.29	Bearing
SGC-OFP-05	108.90	11.85	15.30	13.61	58.42	265.82	Bearing
Average	110.92	11.66	15.86	13.87	59.51	270.76	
			Model-2				
SGC-OFP;WP-01	167.20	14.60	20.00	16.72	89.70	326.54	Bearing
SGC-OFP; WP-02	166.40	14.10	20.20	16.64	89.27	324.98	Bearing
SGC-OFP; WP-03	165.20	13.40	20.30	16.52	88.63	322.64	Bearing
SGC-OFP; WP-04	164.50	12.90	20.50	16.45	88.25	321.27	Bearing
SGC-OFP; WP-05	163.20	12.80	20.60	16.32	87.55	318.73	Bearing
Average	165.30	13.56	20.32	16.53	88.68	322.83	

Table 3. Specimen's characteristic properties of model 3 and model 4

Sample ID.	Ultimate load (kN)	Failure displacement (mm)	K (kN/mm)	Force per bolt (kN)	Compressive strength (N/mm^2)	Bearing stress (N/mm^2)	Mode of failure
			Model-3				
SGC-IFP;OFP-01	158.20	14.15	22.40	19.78	84.87	386.17	Bearing and net tension
SGC-IFP; OFP-02	159.00	14.32	22.20	19.88	85.30	388.12	Bearing and net tension
SGC-IFP; OFP-03	159.50	14.54	22.10	19.94	85.57	389.34	Bearing and net tension
SGC-IFP; OFP-04	160.10	14.72	21.90	20.01	85.89	390.80	Bearing and net tension
SGC-IFP; OFP-05	160.90	14.93	21.80	20.11	86.32	392.76	Bearing and net tension
Average	159.54	14.53	22.08	19.94	85.59	389.44	
			Model-4				
SGC-S-IFP;OFP;WP-B-01	213.20	11.28	26.10	21.32	114.38	415.95	Bearing and net tension
SGC-S-IFP;OFP;WP-B-02	212.40	11.35	25.60	21.24	113.95	414.39	Bearing, net tension, and cleavage
SGC-S-IFP;OFP;WP-B-03	211.50	12.23	24.70	21.15	113.47	412.64	Bearing, net tension, and cleavage
SGC-S-IFP;OFP;WP-B-04	210.30	13.25	24.10	21.03	112.82	410.30	Bearing, net tension, and cleavage
SGC-S-IFP;OFP;WP-B-05	209.80	13.53	23.40	20.98	112.55	409.32	Bearing and net tension
Average	211.44	12.33	24.78	21.14	113.43	412.52	

In the model-1 test samples, the load transfer path from one segment of the connection to the other occurs only in the flange region via the outer flange cover plates and 16 M8 8.8-grade bolts. The average ultimate load of test samples is 110.92 kN, with a stiffness value of 15.86 kN/mm on average. This model's test samples had average bearing stress of 270.76 N/mm^2 per bolt location and average compressive strength of 59.50 N/mm^2. Fig. 3 depicts the failure mode of model-1 and model-2. Model-1 samples bearing displacement lengths ranged from 3 mm to 12 mm, with the upper H-section having longer bearing holes than the lower H-section. The load transfer path from one segment of the connection to the other occurs in both the flange and web region of the model-2 test samples via the outer flange and web cover plates and 20 M8 8.8-grade bolts. The ultimate load of the test samples is 165.30 kN, with a stiffness value of 20.32 kN/mm. The test samples from this model had average bearing stress of 322.80 N/mm^2 per bolt location and average compressive strength of 88.68 N/mm^2 at failure. The length of bearing displacement is recorded to range between 2 mm and 11 mm, and the lower H-section had longer bearing holes than the upper H-section.

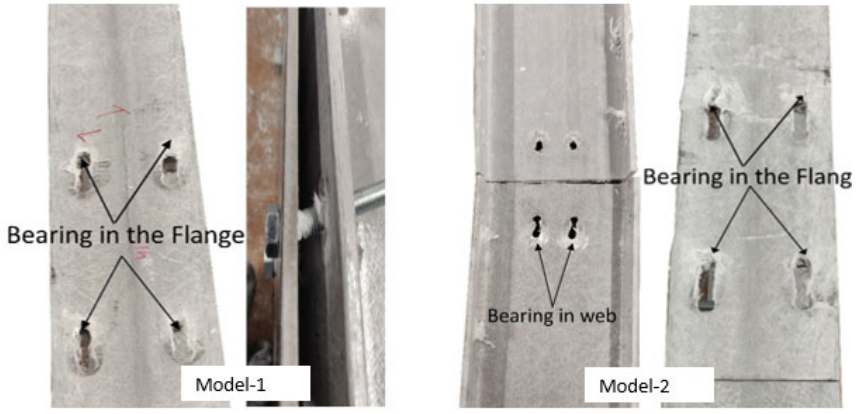

Fig. 3. Failure modes observed in the model-1 and model-2

In the model-3 test samples, the load transfer path from one segment of the connection to the other occurs only in the flange region via the inner and outer flange cover plates and 16 M8 8.8-grade bolts. The ultimate load of the test samples is 159.54 kN, with a stiffness value of 22.08 kN/mm. This model's test samples had average bearing stress of 389.44 N/mm^2 per bolt location and average compressive strength of 85.59 N/mm^2. Fig. 4 depicts the failure mode of model-3 and model-4. The model-3 samples bearing displacement length ranged from 4 mm to 12 mm, with the lower H-section having longer bearing holes than the upper H-section. In the model-4 test samples, the load transfer path occurs in both the flange and web region, as well as 20 M8 8.8-grade bolts. The test samples' average ultimate load is 211.44 kN, with a stiffness value of 24.78 kN/mm. The test samples from this model had average bearing stress of 412.52 N/mm^2 per bolt location and average compressive strength of 113.43 N/mm^2 at failure. The length of bearing displacement was recorded to range between 2 mm and 8 mm, and both the upper and lower H-sections had similar length bearing holes; however, the cleavage cracks that caused failure were predominantly in the lower H-section flange, which displaced the connection's strength and the flange region's weakness. The cleavage cracks formed in the flange region were also affected by the edge value of the bolted connection.

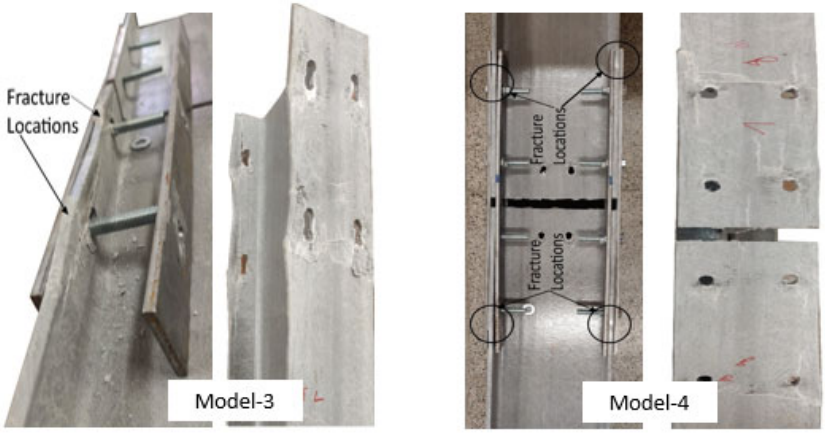

Fig. 4. Failure modes observed in the model-3 and model-4

The un-cut GFRP short columns failed solely due to crushing, and all of the samples had large cracks, primarily at the web and flange junction. The ultimate load and compressive strength of uncut short columns are shown in Table 4. The average ultimate load is 227.74 kN, and the average compressive strength is 122.18 N/mm^2.

Table 4. GFRP controlled sample characteristic properties

Specimen ID	Ultimate load (kN)	Compressive strength (N/mm^2)
1	230.90	123.87
2	228.50	122.59
3	227.30	121.94
4	226.40	121.46
5	225.60	121.03
Average	227.74	122.18

Table 5 shows the average ultimate loads of all the test models, with model-4 exhibiting the highest load tolerance compared to the other three connection models. It should also be noted that the cracks seen in the model-4 test samples are caused by net tension in the flange casing cleavage rather than bold bearing. As a result, failure can be attributed to the material

properties of the GFRP H-sections rather than the strength of the connection. Model-4 specimens also had significantly higher bearing strength compared to other models, as well as greater practical bearing resistance compared to calculated theoretical bearing resistance. In comparison to the un-cut GFRP H-section short column, the model-4 specimen provided 92.83% compressive strength.

Table 5. Summary of model characteristic properties

Model	Ultimate load (kN)	Compressive strength (N/mm^2)	Percentage Compressive strength to un-cut section (%)	Experimental bolt bearing resistance (kN)	Theoretical bolt bearing resistance (kN)
1	110.92	59.51	48.71	13.87	10.11
2	165.30	88.68	72.58	16.53	10.72
3	159.54	85.59	70.05	19.94	12.81
4	211.44	113.43	92.83	21.14	13.18

4. Conclusions

This experimental study investigates the behavior of 20 spliced GFRP no-bearing connections and 5 un-cut GFRP short columns subjected to axial loading. All samples are tested by the BS EN 13706-3 guidelines for testing short columns.

- This experimental study identifies the key design principles that should be considered fundamental for designing GFRP H-section short column non-bearing spliced connections, which are, and the absence of a web cover plate increases the bearing in the flange region due to load transfer from one segment to the other using the flange region only as the load path. This reduces the load-bearing capacity of the joint due to premature failure in the flange region.
- Pitch and edge distances have a significant impact on the load-bearing capacity of the joint and the failure modes of the structure. If the value of the connection's edge is large, the connection can be expected to fail due to bearing failure; this is a valuable aspect in terms of robustness because bearing failure is not abrupt and sudden.
- The test samples from model-4 displayed significant load-bearing capacity with a compressive strength of 92.83% compared to an uncut GFRP short column subjected to axial loading. The joint in the model-4 samples had two outer flange plates, four inner flange plates, two web plates, and 20 M8 8.8-grade bolts. The use of web plates and reinforcement from flange plates in this model significantly reduces the length of bolt bearing and provides a load path through the flange and web region, which contributes significantly to the joint's load-bearing capacity of 211.44 kN on average.
- Failure in model-4 samples was not sudden or abrupt, as evidenced by the load versus displacement graph of this model; it can also be deduced that these test samples provided the least elastic deformation when compared to other models, with an average stiffness of 24.7 kN/mm.
- Although the un-cut GFRP short column had higher compressive strength than the samples from model-4, which was approximately 7% higher on average, model-4 can be considered a good alternative for using or connecting short columns in GFRP structures.

The study focuses solely on axial loading conditions on short column connections, but when implemented in real-time, other eccentric loadings play an important role in the connection's strength. The load tolerance and characteristics of the model-4 test samples were as good as or better than an un-cut GFRP short column. Further design improvements, such as thicker cover plates, staggered bolt connections, increased edge value, and use of GFRP bolts to reduce bearing, should be investigated.

Acknowledgement

The authors appreciate the assistance provided by REVA University during the testing process.

References

Al-Rubaye, M., Manalo, A., Alajarmeh, O., Ferdous, W., Lokuge, W., Benmokrane, B., & Edoo, A. (2020). Flexural behaviour of concrete slabs reinforced with GFRP bars and hollow composite reinforcing systems. *Composite structures*, *236*, 111836.

Bazli, M., Zhao, X. L., Jafari, A., Ashrafi, H., Bai, Y., Raman, R. S., & Khezrzadeh, H. (2020). Mechanical properties of pultruded GFRP profiles under seawater sea sand concrete environment coupled with UV radiation and moisture. *Construction and Building Materials*, *258*, 120369.

BSI. (2002). BS EN 13706-3: Reinforced plastic composites–Specification for pultruded profiles–Part 3: Specific requirements.

BSI. (2002). BS EN 1990: 2002: Eurocode–Basis of structural design.

En, B. S. (1991). 1-1: 2002 Eurocode 1: Actions on structures—General actions—Densities, self-weight, imposed loads for

buildings.
EN, C. (1993). 1-9, Eurocode 3: Design of steel structures. *fatigue*.
Fahmy, M. F. M. (2013). Advanced fiber-reinforced polymer (FRP) composites to strengthen structures vulnerable to seismic damage. In *Advanced Fibre-Reinforced Polymer (FRP) Composites for Structural Applications* (pp. 511-551). Woodhead Publishing.
Ferdous, W., Manalo, A., AlAjarmeh, O., Mohammed, A. A., Salih, C., Yu, P., & Schubel, P. (2021). Static behaviour of glass fibre reinforced novel composite sleepers for mainline railway track. *Engineering Structures*, *229*, 111627.
Frigione, M., & Lettieri, M. (2018). Durability issues and challenges for material advancements in FRP employed in the construction industry. *Polymers*, *10*(3), 247.
Harley, G. L., Maxwell, J. T., Holt, D., & Speagle, C. B. (2017). Construction history of the deason house, jones county, mississippi. *Dendrochronologia*, *43*, 50-58.
Kim, Y. J. (2019). State of the practice of FRP composites in highway bridges. *Engineering Structures*, *179*, 1-8.
Liu, T., Liu, X., & Feng, P. (2020). A comprehensive review on mechanical properties of pultruded FRP composites subjected to long-term environmental effects. *Composites Part B: Engineering*, *191*, 107958.
Mara, V., Haghani, R., & Al-Emrani, M. (2016). Improving the performance of bolted joints in composite structures using metal inserts. *Journal of composite materials*, *50*(21), 3001-3018.
Nhut, P. V., Yoresta, F. S., Kitane, Y., Hashimoto, K., & Matsumoto, Y. (2021). On the strengthening of pultruded GFRP connections using glass fiber sheets: A study on the influence of bolt diameter. *Applied Composite Materials*, 1-31.
Phan Viet, N., Kitano, Y., & Matsumoto, Y. (2020). Experimental investigations of the strengthening effects of CFRP for thin-walled storage tanks under dynamic loads. *Applied Sciences*, *10*(7), 2521.
Russo, S. (2019). On failure modes and design of multi-bolted FRP plate in structural joints. *Composite Structures*, *218*, 27-38.
Sheikh, S. A., & Li, Y. (2007). Design of FRP confinement for square concrete columns. *Engineering Structures*, *29*(6), 1074-1083.
Shin, Y. H., Yoong, Y. Y., Hejazi, F., & Saifulnaz, M. R. (2019, November). Review on pultruded FRP structural design for building construction. In *IOP Conference Series: Earth and Environmental Science* (Vol. 357, No. 1, p. 012006). IOP Publishing.
Standards, E. (n.d.). BS EN 15048-1:2016 Non-preloaded structural bolting assemblies. *General requirements*.
Tempelman, E. (2014). Lightweight materials, lightweight design?. In *Materials experience* (pp. 247-258). Butterworth-Heinemann.
Vedernikov, A., Safonov, A., Tucci, F., Carlone, P., & Akhatov, I. (2020). Pultruded materials and structures: A review. *Journal of Composite Materials*, *54*(26), 4081-4117.
Viet, N. P., Yoresta, F. S., Kitane, Y., Hashimoto, K., & Matsumoto, Y. (2021). Improving the shear strength of bolted connections in pultruded GFRP using glass fiber sheets. *Composite Structures*, *255*, 112896.
WALLACE, H. (1965). STRUCTURAL DESIGN. *Architectural Science Review*, *8*(1), 5-8.
Zhao, X. L., & Zhang, L. (2007). State-of-the-art review on FRP strengthened steel structures. *Engineering structures*, *29*(8), 1808-1823.